The influence of finely layered seabeds on acoustic propagation in shallow water

Alec J DUNCAN[1]; Alexander N GAVRILOV[2], Matthew W KOESSLER[3]

Centre for Marine Science and Technology, Curtin University, Australia

ABSTRACT

Except in the deep ocean, the seabed has a major influence on low-frequency acoustic propagation. The formulation of an adequate geoacoustic model of the seabed is therefore one of the most important tasks facing anyone carrying out acoustic propagation modelling to predict underwater sound levels in coastal and continental shelf waters. It is often assumed that seabed layering on scales significantly smaller than the acoustic wavelength can be ignored when carrying out such modelling, and that these layers can instead be replaced by a simplified model involving a small number of layers in which the geoacoustic parameters vary smoothly with depth. This paper explores this assumption, with particular reference to the finely layered elastic seabeds typical of the Australian continental shelf. This investigation is based on a comparison of the plane-wave reflection coefficient vs grazing angle curves of these two representations of the seabed.

Keywords: Underwater, Sound, Propagation, Shallow water, Layered seabed I-INCE Classification of Subjects Number: 54.3

1. INTRODUCTION

Seabeds often consist of layered geological strata that have arisen as a result of sedimentary deposition in different climatic conditions. This is particularly apparent in the case of Australia's carbonate continental shelves, which have undergone varying degrees of cementation during periods of low sea level, resulting in strong acoustic impedance contrasts between layers that can vary from several metres to less than one metre thick (1). In these seabeds, material properties can vary abruptly between those of completely unconsolidated sand and those of a well-cemented soft limestone known as calcarenite, with layers having intermediate properties also occurring. A further consequence of the manner in which these seabeds are formed is that it is common to have an unconsolidated layer underlying a cemented layer, resulting in a sudden reduction in compressional and shear wave speeds with increasing depth into the seabed. A bit further down there may be an equally sudden increase in wave speeds due to another cemented layer. These sudden reductions and increases in wave speeds tend to be superimposed on a general increase in speed with increasing depth that results from compaction due to the increasing overburden pressure.

It would be very unlikely that a numerical modeller intent on modelling acoustic propagation in such an environment would have access to the detailed geological and geoacoustic data necessary to construct an accurate geoacoustic model of a seabed like this. Instead, it is usually necessary to approximate the true, finely layered seabed, with an approximate seabed consisting of a small number of layers with geoacoustic properties chosen to give a similar acoustic reflectivity.

In this paper we look at how such an equivalent seabed model could be derived and investigate the validity of this approximate approach for a specific example. We restrict ourselves to horizontally stratified media (i.e. ignore dip of the strata), and consider only the plane wave reflection coefficient at the water-seabed interface. Effects not captured by the plane wave reflection coefficient, such as

[1] a.duncan@cmst.curtin.edu.au
[2] a.gavrilov@cmst.curtin.edu.au
[3] matthew.koessler@postgrad.curtin.edu.au

lateral (Head) waves and interface waves can be important in some circumstances, but are not considered here.

2. THEORY

The theoretical basis for modelling the propagation of elastic waves in layered rock strata has been well studied for many years because of its importance to seismology, and is detailed in a number of textbooks, for example references (2, 3, 4, 5, 6).

Brekhovskikh and Godin (5) deal specifically with the case of a horizontally stratified medium in which the layers are much thinner than the wavelengths involved, and provide formulae for the elastic properties of an equivalent medium. They point out several interesting effects of the layering:

- The equivalent medium is anisotropic, i.e. the speeds of compressional (*P*), vertically polarised shear (*SV*), and horizontally polarised shear (*SH*) waves are functions of the directions in which the waves are travelling.
- The speeds of *SV* and *SH* waves are different.
- There is continual conversion back and forth between *P* and *SV* waves.

Brekhovskikh and Godin give the elastic constants of an anisotropic medium equivalent to a repeating stack of thin layers in terms of the depth dependent Lamé constants, λ and μ, and the density, ρ, in the layer stack as:

$$\tilde{\lambda} = 2\left\langle \lambda\mu(\lambda+2\mu)^{-1} \right\rangle + \frac{\left\langle \lambda(\lambda+2\mu)^{-1} \right\rangle^2}{\left\langle (\lambda+2\mu)^{-1} \right\rangle}, \quad \tilde{\lambda}' = \frac{\left\langle \lambda(\lambda+2\mu)^{-1} \right\rangle}{\left\langle (\lambda+2\mu)^{-1} \right\rangle} \tag{1}$$

$$\tilde{\mu} = \langle \mu \rangle, \quad \tilde{\mu}' = \frac{\left\langle \mu(\lambda+2\mu)^{-1} \right\rangle}{\left\langle (\lambda+2\mu)^{-1} \right\rangle}, \quad \tilde{\mu}'' = \langle 1/\mu \rangle^{-1}, \quad \tilde{\rho} = \langle \rho \rangle \tag{2}$$

where $\langle f \rangle = \dfrac{1}{h}\displaystyle\int_0^h f(z)dz$ is the average over the layer stack.

A plane wave in the water column incident onto the seabed only gives rise to compressional and vertically polarised shear waves in the sediments, so horizontally polarised shear waves are not considered further in this paper. According to Brekhovskikh and Godin the vertical components of the wave vectors for *P* and *SV* waves in an anisotropic medium of this type are given by:

$$\alpha^2 = \frac{-b \pm \sqrt{b^2 - 4a\tilde{\mu}''\left(\tilde{\lambda}' + 2\tilde{\mu}'\right)}}{2\left(\tilde{\lambda}' + 2\tilde{\mu}'\right)\tilde{\mu}''}, \tag{3}$$

where:

$$a = \left\{\xi^2\left(\tilde{\lambda} + 2\tilde{\mu}\right) - \rho\omega^2\right\}\left(\tilde{\mu}''\xi^2 - \rho\omega^2\right),$$

$$b = \xi^2\left\{\left(\tilde{\lambda} + 2\tilde{\mu}\right)\left(\tilde{\lambda}' + 2\tilde{\mu}'\right) + \left(\tilde{\mu}''\right)^2 - \left(\tilde{\lambda}' + \tilde{\mu}''\right)^2\right\} - \rho\omega^2\left(\tilde{\lambda}' + 2\tilde{\mu}' + \tilde{\mu}''\right),$$

ω is angular frequency, and ξ is the horizontal component of the wave vector, which by Snell's Law is the same for the acoustic wave in the water column, and both the compressional and shear waves in the seabed.

The positive sign on the right hand side of Equation 3 gives α_{sv}, the vertical component of the wave vector of the *SV*-wave, and the negative sign gives α_p, the vertical component of the wave vector of the *P*-wave.

Horizontally and vertically travelling compressional waves have phase speeds of:

$$c_p^{(1)} = \sqrt{\frac{\tilde{\lambda} + 2\tilde{\mu}}{\tilde{\rho}}}, \text{ and} \tag{4}$$

$$c_p^{(3)} = \sqrt{\frac{\tilde{\lambda}' + 2\tilde{\mu}'}{\tilde{\rho}}} \tag{5}$$

The superscripts (1) and (3) refers to the horizontal (X), and vertical (Z) directions respectively.

Vertically polarised shear waves travelling both horizontally and vertically (but not at intermediate angles) have a phase speed of:

$$c_{sv}^{(1)} = c_{sv}^{(3)} = \sqrt{\frac{\tilde{\mu}''}{\tilde{\rho}}}, \tag{6}$$

Imposing the usual fluid-solid boundary conditions of continuity of normal velocity and continuity of normal stress at the water-seabed interface leads to the following expression for the plane wave pressure reflection coefficient:

$$R = \frac{Z_n - Z}{Z_n + Z}, \tag{7}$$

where:

$$Z = \frac{\rho_0 \omega}{\sqrt{k_0^2 - \xi^2}}, \quad Z_n = \frac{i\left(\tilde{\lambda}' + 2\tilde{\mu}'\right)\alpha_p v_3^{(1)} - \tilde{\lambda}'\xi^2 + \alpha_{sv} A\left\{i\left(\tilde{\lambda}' + 2\tilde{\mu}'\right)v_3^{(3)} + \tilde{\lambda}'\xi\right\}}{i\omega\left(v_3^{(1)} + A v_3^{(3)}\right)},$$

$$A = \frac{\xi\left(\alpha_p - i v_3^{(1)}\right)}{\alpha_{sv}^2 + i\xi v_3^{(3)}}, \quad v_3^{(1)} = i\frac{\rho\omega^2 - \left(\tilde{\lambda} + 2\tilde{\mu}\right)\xi^2 - \tilde{\mu}''\alpha_p^2}{\alpha_p\left(\tilde{\lambda}' + \tilde{\mu}''\right)}, \quad v_3^{(3)} = -i\frac{\rho\omega^2 - \left(\tilde{\lambda} + 2\tilde{\mu}\right)\xi^2 - \tilde{\mu}''\alpha_{sv}^2}{\xi\left(\tilde{\lambda}' + \tilde{\mu}''\right)}.$$

ρ_0 and k_0 are the density and acoustic wavenumber in the water column respectively.

3. RESULTS AND DISCUSSION

For illustrative purposes, we consider a seabed consisting of alternating layers of well-cemented calcarenite and semi-cemented sand/calcarenite with the geoacoustic properties given in Table 1. The water column was modelled to be isovelocity with a sound speed of 1500 m.s^{-1} and a density of 1024 kg.m^{-3}.

Table 1 - Seabed geoacoustic properties used in this study

	Well-cemented calcarenite	Semi-cemented sand/calcarenite
Layer thickness (m)	1.0	1.0
Density (kg.m^{-3})	2200	1900
Compressional wave speed (m.s^{-1})	2600	2100
Compressional wave absorption (dB/wavelength)	0.2	0.12
Shear wave speed (m.s^{-1})	1200	550
Shear wave absorption (dB/wavelength)	0.4	0.25

The equivalent anisotropic medium properties for this seabed were calculated using equations (1) and (2). Equation (3) was then used to evaluate the vertical components of the wave vectors of the P

and *SV* waves as a function of their horizontal components, allowing the wave speeds in the seabed to be computed. These wave speeds are plotted in Figure 1 as a function of the grazing angle of each of these waves in the seabed.

The *P*-wave has a speed of 2378 m.s^{-1} when propagating horizontally (0°) and 2287 m.s^{-1} when propagating vertically (90°), however the minimum wave speed is 2246 m.s^{-1}, which occurs for a wave propagating at a grazing angle of 53°

The *SV*-wave has a minimum speed of 689 m.s^{-1} when propagating at grazing angles of both 0° and 90°, and a maximum speed of 916 m.s^{-1} when propagating at 45°.

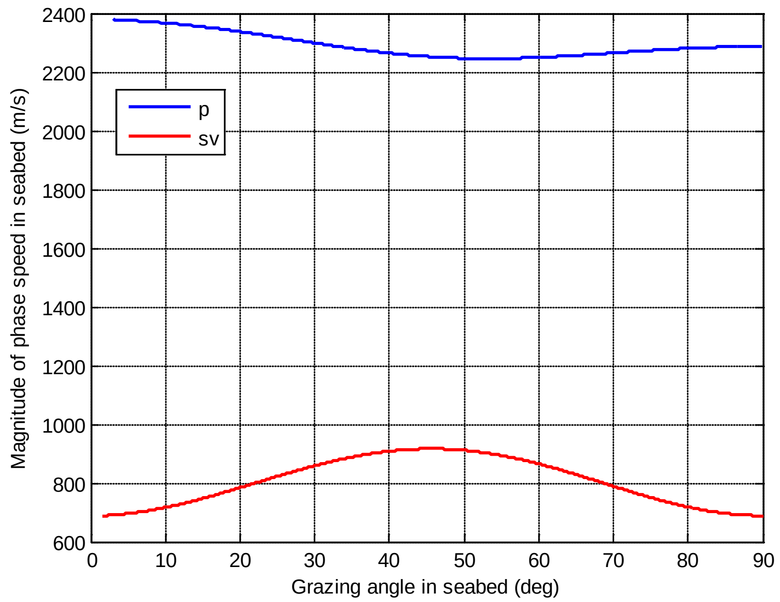

Figure 1. Compressional (*P*) and vertically polarised shear (*SV*) wave speeds as a function of the direction of the corresponding wave-vector in the seabed.

In Figure 2 we consider the *P* and *SV* waves produced by the interaction of a plane acoustic wave in the water column with the seabed. The wave speeds are plotted here as a function of the grazing angle of the incident wave. Note that the critical angle for the *P*-wave corresponds to a wave travelling horizontally in the seabed, and is therefore determined by the horizontal compressional wave speed given by Equation (4), which in this case equates to a critical angle of 50.8°. The *P*-wave speeds are shown in Figure 2 only for propagating waves in the seabed, which correspond to incident grazing angles greater than the critical angle.

It can be seen that the *P*-wave speed has its minimum at an incident grazing angle of 67° and its maximum at the critical angle.

The *SV*-wave speed varies monotonically between a minimum of 689 m.s^{-1} at normal incidence, and a maximum of 902 m.s^{-1} at grazing incidence.

Figure 3 shows the plane wave reflection coefficient for the equivalent anisotropic seabed computed using Equation 7, and compares this to the plane wave reflection coefficient for an isotropic seabed with the same density as the anisotropic seabed, a compressional wave speed equal to the horizontal compressional wave speed in the anisotropic seabed, and the shear wave speed that gave the best match between the two sets of curves. The isotropic seabed reflection coefficient was calculated using the usual equation for the reflection coefficient for an isotropic halfspace (see Reference 5). The isotropic seabed shear speed was initially set to the value read from Figure 2 for an incident grazing angle of 30°, and then adjusted manually to obtain the best apparent match between reflection coefficient magnitudes for grazing angles between 0° and 50°. (Increasing the shear speed deepens the dip in the reflection coefficient that occurs in this angle range and vice-versa.) The resulting geoacoustic properties are listed in Table 2. In Figure 3 there are differences in detail, but it can be seen that in terms of plane wave reflection coefficients, the isotropic medium provides a very good approximation to the true anisotropic case.

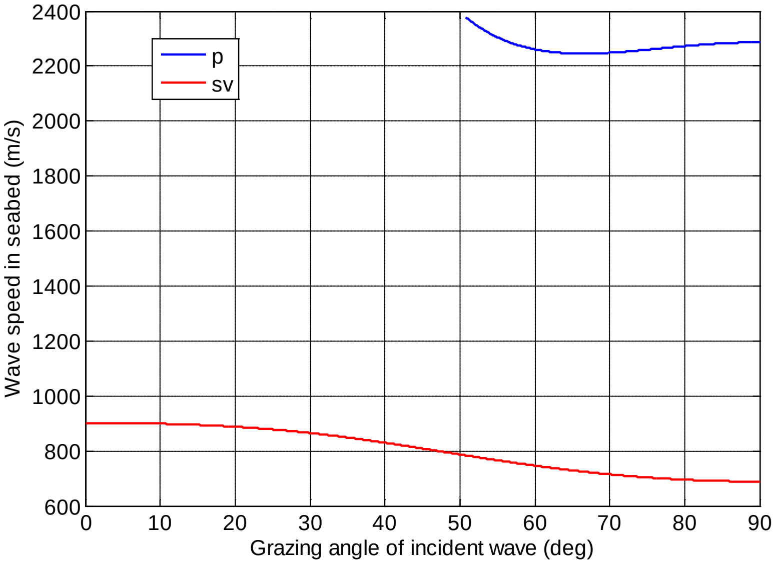

Figure 2 - Compressional wave and vertically polarised shear wave speeds in the seabed as a function of the grazing angle of the incident wave in the water column.

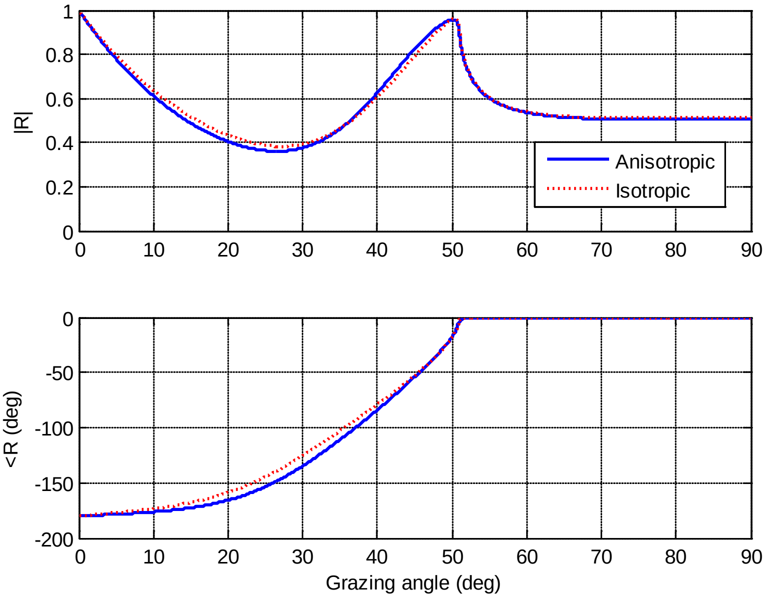

Figure 3. Magnitude and phase of the plane wave pressure reflection coefficient as a function of grazing angle for the anisotropic and isotropic seabed models discussed in the text.

Table 2 - Isotropic seabed geoacoustic properties

Density (kg.m^{-3})	2050
Compressional wave speed (m.s^{-1})	2378
Compressional wave absorption (dB/wavelength)	0.12
Shear wave speed (m.s^{-1})	880
Shear wave absorption (dB/wavelength)	0.45

To check how well the equivalent anisotropic medium model by Brekhovskikh and Godin compares to a direct numerical solution for a layered bottom, the reflection coefficient calculation program

BOUNCE (7) was run at a number of different frequencies for a seabed consisting of 100 repetitions of the two layer stack described in Table 1, overlying a halfspace with the isotropic medium properties given above. The result shown in Figure 4 demonstrates that Equation (7) provides a good estimate of the average reflection coefficient, but that there is some variation around this due to frequency dependent interference effects occurring within the seabed.

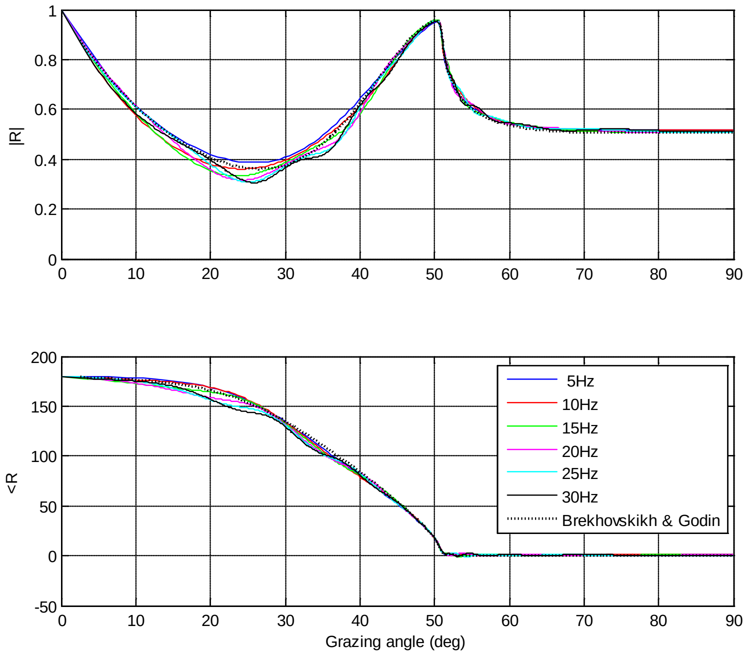

Figure 4. Magnitude and phase of the plane wave reflection coefficient computed by BOUNCE at the indicated frequencies for a seabed consisting of 100 repetitions of the two-layer sequence described in Table 1 over a halfspace with the isotropic medium properties described in the text, compared to the Brekhovskikh and Godin equivalent model given by Equation (7).

Fourier synthesis (8) was used to determine the waveform of the reflected wave due to an incident plane wave with the waveform shown in Figure 5. A grazing angle of 25° was chosen as this gave the largest discrepancies in Figure 4. The incident waveform was defined by the equation :

$$s(t) = \begin{cases} \sin(2\pi f_c t) - \frac{1}{2}\sin(4\pi f_c t), & 0 < t < 1/f_c \\ 0, & \text{elsewhere} \end{cases} \tag{8}$$

with $f_c = 20$ Hz.

The Fourier synthesis results were based on numerical reflection coefficients calculated using BOUNCE at 1 Hz increments from 1 Hz to 100 Hz, and on analytic reflection coefficients obtained from Equation (7) for an anisotropic halfspace, and the usual equation for the reflection coefficient for an isotropic halfspace (see Reference 5). Although frequency appears explicitly in Equation (7) the reflection coefficients evaluated using this equation are frequency independent.

The computed reflected waveforms are compared in Figure 6. There are slight differences in the amplitudes of the initial impulses but the main difference between the waveforms is a second arrival in the numerical result that does not occur in either of the analytic results. The timing of this second pulse is consistent with it being due to a reflection of shear waves from the top of the halfspace that underlies the alternating layers. It is likely that the differences between the reflection coefficient curves shown in Figure 4 are due to the same mechanism, which leads to the conclusion that these differences are due to limitations of the numerical model in only being able to represent a finite number of layers, rather than being a real effect for an infinite sequence of layers.

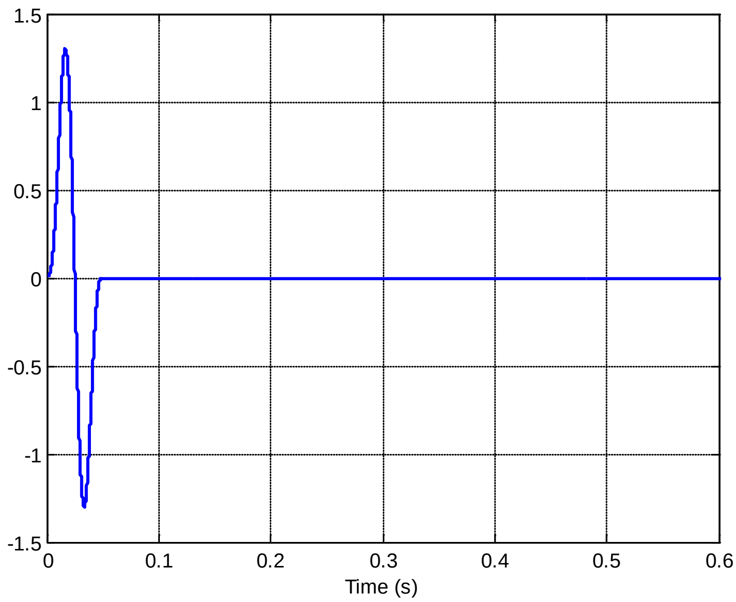

Figure 5. Incident waveform used for Fourier synthesis.

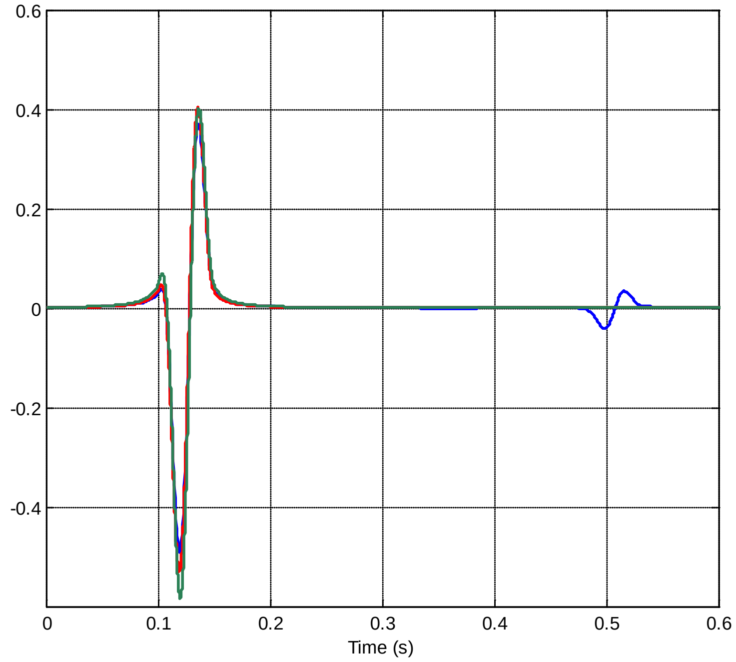

Figure 6. Waveform of reflected wave calculated by Fourier synthesis using numerically calculated reflection coefficients obtained from BOUNCE (blue), equivalent anisotropic seabed (Equation (7), red), and equivalent isotropic seabed (green).

4. CONCLUSIONS

In the example considered here, the plane wave pressure reflection coefficient of a seabed consisting of a repeating stack of thin layers is well represented by Equation (7), which is derived from the equivalent anisotropic seabed model representation of Brekhovskikh and Godin (5).

It was also possible to find parameters for an isotropic seabed model that gave a very similar reflection coefficient curve to the anisotropic seabed model and would be more suitable for inclusion in numerical acoustic propagation models. The isotropic model parameters were obtained by using the same density, matching the compressional wave speed to the horizontal compressional wave speed of the anisotropic seabed, and by adjusting the shear speed until the best match between reflection coefficient curves was obtained.

Further work needs to be done to explore the limitations of these approximations and to establish whether the good match between plane wave reflection coefficient curves carries through to other effects not captured by the reflection coefficient such as lateral and interface waves.

REFERENCES

1. James NP, Bone Y. Neritic Carbonates Sediments in a Temperate Realm: Southern Australia. New York, USA. Springer, 2011.
2. Ewing WM, Jardetzky WS, Press F. Elastic Waves In Layered Media. New York, USA. McGraw-Hill, 1957.
3. Brekhovskikh, LM. Waves In Layered Media. New York, USA. Academic Press, 1960.
4. Kennett BLN. Seismic wave propagation in stratified media. Cambridge, UK. Cambridge University Press, 1983.
5. Brekhovskikh LM, Godin OA. Acoustics of Layered media I - Plane and Quasi-Plane Waves. Berlin-Heidelberg, Germany. Springer-Verlag, 1990.
6. Brekhovskikh LM, Godin OA. Acoustics of Layered media II - Point Sources and Bounded Beams. Berlin-Heidelberg, Germany. Springer-Verlag, (1992)
7. Porter MB. Acoustics Toolbox, from: http://oalib.hlsresearch.com/FFP/index.html.
8. Jensen FB, Kuperman WA, Porter MB, Schmidt H. Computational Ocean Acoustics. 2nd ed. New York, USA. Springer, 2011.